RAPID COMMUNICATIONS

PHYSICAL REVIEW B VOLUME 45, NUMBER 7 15 FEBRUARY 1992-I

Edge magnetoplasmons in the time domain

R. C. Ashoori, H. L. Stormer, L. N. Pfeiffer, K. W. Baldwin, and K. West
AT&T Bell Laboratories, Murray Hill, New Jersey 07974
(Received 7 October 1991)

We have studied edge magnetoplasmons (EMP's) created by pulses of 100 ps width in a high-mobility two-dimensional electron gas, using a cryogenic transistor. We find that magnetoplasmon motion along the edge occurs only in the direction expected for negatively charged electrons; there is no hint of propagation in the opposite direction expected for positively charged quasiholes. We also measure the periods and decay rates of the edge modes continuously as a function of the magnetic field. From these characteristics we deduce the width of the EMP boundary layer as well as the magnetic-field-dependent momentum-relaxation time.

Plasma oscillations in the two-dimensional electron gas (2DEG) are known to have low-frequency modes associated with the edge of the sample. These edge magnetoplasmons (EMP's) in the 2DEG in both semiconductors and on the surface of liquid helium have received much attention in recent years. All experimental studies to date have been in the frequency domain.[1-10] However, the propagation of edge magnetoplasmon can be directly recorded by modern sampling oscilloscopes. An advantage of such a technique is the ability to determine the *direction* of edge magnetoplasmon travel. It has been proposed[11] that the edge magnetoplasmon response of the 2DEG may be an effective probe of edge effects in the fractional quantum Hall effect especially if the direction of plasmon propagation can be determined. In this paper, we present results of a study in which the time response of the edge of a 2DEG to a short pulse is investigated. An on-chip cryogenic high-electron-mobility transistor (HEMT) has given the requisite sensitivity.

Two features of this experiment, the ability to make measurements in the time domain and the high sensitivity of our apparatus, have produced two main results. First, EMP's travel only in the direction given by the $e\mathbf{B}\times\mathbf{N}$ drift of electrons at the edge of the sample (with $\mathbf{N}$ the outward normal at the edge of the 2D gas). No EMP propagation in the opposite direction, corresponding to the existence of carriers of the opposite sign, is observed. Second, our technique allows continuous measurement of the EMP round-trip times and decay rates as a function of Landau-level filling factor from 0.4 to 13 T. Using the "boundary layer" theory of Volkov and Mikhailov,[12] we obtain from these results both an independent measure of the momentum relaxation time and the boundary layer width.

We have studied EMP's in three different 2DEG samples. These samples, A, B, and C, had densities of 1.2, 1.5, and 1.9×10^{11} cm^{-2}, respectively, and mobilities of 6.2×10^{6}, 6.4×10^{6}, and 2.1×10^{6} cm^{2}V^{-1}s^{-1}, respectively. The inset of Fig. 1 provides a schematic of the geometry. Circular mesas of 540 μm diameter are etched on the samples. The mesas are about 1 μm tall and are defined in the center of a large piece of 500-μm-thick GaAs. Two gates 10×10 μm^2 are evaporated over the edge of the mesas. One of these we refer to as the "pulser," to which fast electric pulses (typically 100 ps, 50 mV) are applied. The other is the "detector" which is electrically connected via a 300-μm-long stripline to the gate of an on-chip HEMT of bandwidth ≈ 12 GHz and 0.3 pF gate capacitance. The transistor allows us to detect fluctuations in charge at the 2DEG of as few as 100 electrons under the detector on a sub nanosecond time scale. It is mounted in a fashion that leaves its operation practically unaffected by the magnetic field applied to the sample. Each mesa contains two center contacts for *in situ* measurement of σ_{xx}.

The gates can be independently biased with respect to the 2DEG. At each value of the magnetic field, after a pulse has been applied, we take two time traces of the output of the transistor on a high-speed oscilloscope (Tektronix 11801). First, biases are set to deplete the 2DEG of electrons under both gates (confirmed through capacitance measurements); and second, zero-bias is applied between the gates and the 2DEG. By subtracting these two traces, we are left with the signal associated with the 2DEG and reject direct crosstalk between the gates. All

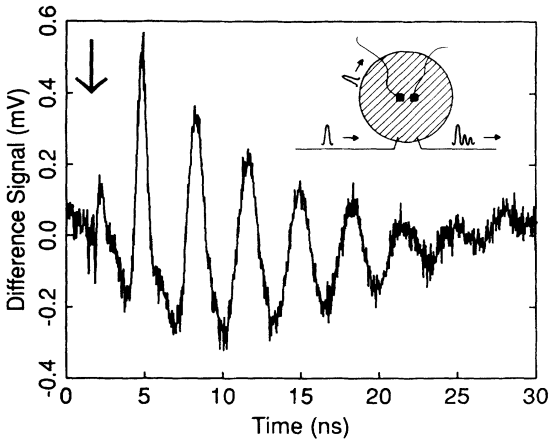

FIG. 1. The response at the detector of sample A to a 100-ps pulse at the pulser. The arrow indicates the application of the pulse. The data are taken at 5.1 T ($\nu=1$) and for a magnetic-field direction in which electrons are forced to take the "long route" between the pulser and the detector. The inset depicts the operation of the sample.

data are taken at 0.3 K.

In Fig. 1, we plot the time trace for a sample with pulser and detector spaced 100 μm apart along the edge of the disk. Due to the circular geometry of the sample, the EMP pulse passes repeatedly under the detector, leading to a periodic signal which decays in time. The sample is in the $\nu=1$ quantum Hall plateau, and the magnetic-field direction is chosen so that electrons must first travel the "long way" around the ring from the pulser to the detector. About 4 ns after a 50 mV, 100-ps-wide positive pulse, is applied to the pulser, a first pulse is received at the detector. This pulse is broader than the excitation pulse (with a width of ≈ 800 ps) and has the polarity appropriate for excess negative charge passing underneath the detector. The pulse clearly broadens further with successive trips around the ring, confirming the dispersive behavior of the EMP's.[9]

The two curves shown in Fig. 2 are from sample C with the 2DEG in the $\frac{2}{3}$ fractional quantum Hall effect (FQHE) regime and two opposite directions of the applied magnetic field. For this sample, the pulser and detector gates are spaced by $\frac{1}{3}$ of the circumference of the mesa. The two curves represent the short and the long paths for pulses traveling between these two gates, and a temporal shift of $\frac{1}{3}$ of the period of oscillation between both traces is clearly visible. Both curves show an exponential decrease in peak heights with time, with the same decay rate.

One of the motivations for the present study derives from the proposal that the FQHE may generate fractionally charged "quasiholes" of charge $+\frac{1}{3}$. MacDonald[13] predicts that a quasihole edge state should arise at $\nu=\frac{2}{3}$. Wen[11] has suggested that quasihole edge states may give rise to EMP excitations which travel in a direction opposite to that expected for electrons. On the other hand, recent nonlocal transport studies[14] of the FQHE hint that edge currents are only carried by electrons.

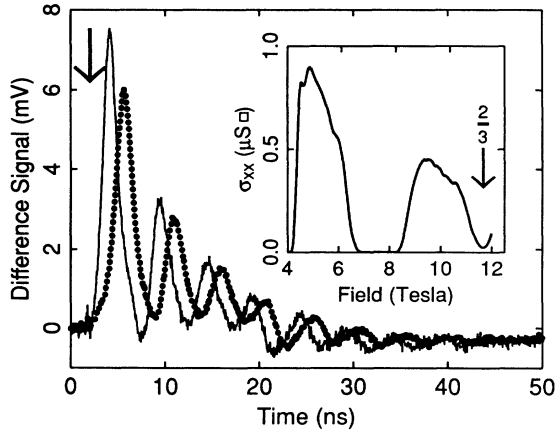

FIG. 2. The pulse responses of sample C in the $\nu=\frac{2}{3}$ FQHE minimum. The pulser and the detector are separated by $\frac{1}{3}$ of the circumference of the mesa. The solid curve is for the magnetic-field orientation such that electronic disturbances take the short path between pulser and the detector; the dotted curve is for the opposite direction of magnetic field. Inset: σ_{xx} as measured on sample C.

Our traces show no features which can be ascribed to motion of charge in the direction opposite to the usual EMP direction. In the trace in which electrons are forced to travel first the "long route" around the mesa ($\frac{2}{3}$ of the circumference) between the pulser and the detector, no features can be seen to precede similar features in the trace taken in the opposite direction of field. In other words, no charge disturbance appears to travel the "short route" between pulser and detector in the case in which electrons are forced to take the long route. This is true for all values of magnetic field. Experiments on sample B give the same result.

We have performed identical measurements on large samples (several mm^2) where the pulser and the detector are closely spaced (50 μm). These samples contain large indium Ohmic contacts to the 2DEG at the sample edge opposite to the gates which absorb all EMP disturbances. This geometry is thus ideally suited to separate EMP pulses traveling in opposite directions. The contrast between the observation of a strong EMP pulse in one magnetic-field direction and the absence of any signal in the opposite field direction at all field values further indicates that either quasihole edge states do not exist or excitations in them do not survive long enough to be observed at the detector.

The high sensitivity and bandwidth of the experimental technique allows us to determine the periods and the damping of the EMP quasicontinuously over a wide magnetic-field range from 0.4 to 13 T. Figure 3 shows the decay rates in sample A as well as the dc conductivity, σ_{xx}, taken *in situ* at 0.3 K. We plot data only up to 6 T to focus on this structured part of the decay rate, as it is relatively featureless beyond this point, with only one more minimum in the EMP damping at the $\nu=\frac{2}{3}$ FQHE state. There is a striking similarity between the EMP decay rate and σ_{xx}. The minima in the decay rate fall at the same positions as the minima in σ_{xx} indicating that the 2DEG density at the sample edge where the EMP propagates is the same as at the sample center. Except at the minima of σ_{xx} there is only small distortion in the shape of the

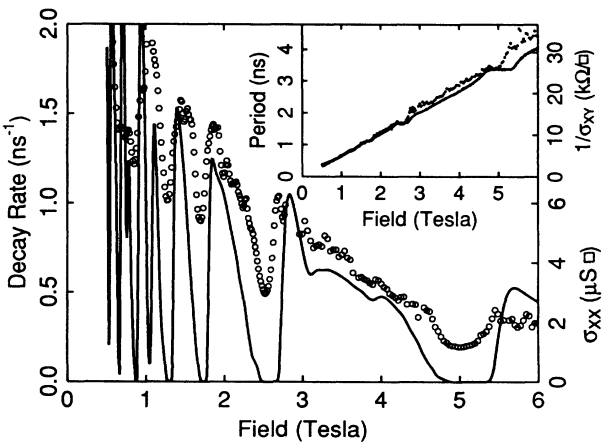

FIG. 3. The decay rate of the EMP in sample A as a function of magnetic field (circles). The solid line is σ_{xx} measured on the same sample. The inset shows the period of the fundamental EMP mode (points) and $1/\sigma_{xy}$.

damping curve when compared with σ_{xx}.

In the inset of Fig. 3 we present the complementary data on the EMP period and compare it with $1/\sigma_{xy}$ obtained from ρ_{xx} and ρ_{xy} measurements on a separate specimen on the same wafer. In agreement with past experimental observations,[4,8] departures from strict proportionality to $1/\sigma_{xy}$ are seen.

At present, there exists no theory predicting damping and frequency of the EMP that includes the effects of edge states and the nonlocal nature of σ_{xx} and σ_{xy} in the QHE regime. We therefore proceed to analyze our data using available classical theories.

Recent models describe the EMP as a nonequilibrium charge disturbance which forms at a boundary layer at the sample edge.[3,12,15] Volkov and Mikhailov[12] (VM) have derived an exact solution to the classical EMP problem for an ideal sample in which σ_{xx} and σ_{xy} are uniform inside and drop to zero in a steplike fashion at the sample edge. They arrive at a single equation [Eq. (41) of Ref. 12],

$$\omega(k)+i\omega'(k)=\frac{2k\sigma_{xy}}{\bar{\epsilon}}\left[\ln\left(\frac{2}{kl}\right)+1\right], \tag{1}$$

relating the frequency ω and the decay rate ω' of EMP modes to the parameters of the 2DEG. Here k is the magnitude of the wave vector of the excitation (which, for the fundamental is given by 2π divided by the mesa circumference) and $\bar{\epsilon}$ is the effective dielectric constant which depends on the structure and environment of the sample. Finally, l depends on the complex conductivity of the sample and is given by

$$l=2\pi i\sigma_{xx}(\omega)/\bar{\epsilon}\omega\,. \tag{2}$$

Physically, the length $|l|$ is identified by VM as the width of the boundary layer.

Equation (1) may be inverted so that our measurements of ω and ω' (as in Fig. 3) directly yield the magnetic-field dependence of l. This inversion can only be performed reliably if the other parameters in Eq. (1) are sufficiently well known. In particular, since l appears in the logarithm of Eq. (1), slight variations in the prefactor can require large changes in l. Both the wave number k (for the fundamental mode) and σ_{xy} are known to high accuracy leaving the largest uncertainty to the value of the dielectric constant.

For two semi-infinite half spaces containing a 2DEG and its edge at their common interface, the value of $\bar{\epsilon}$ is simply the mean of ϵ of both half spaces. Our mesa closely resembles this case and $\bar{\epsilon}=(\epsilon_{\mathrm{GaAs}}+1)/2$ should provide an excellent approximation. However, the procedure is questionable for use in analyses of most other experiments in which the 2DEG is bounded by cleaved edges.[4,9] $\bar{\epsilon}$ is also influenced by metallic objects at distances less than $1/k$ to the sample. This was recently demonstrated by Grodnensky, Heitmann, and von Klitzing[10] (GHvK) who experimentally determined values of $\bar{\epsilon}$ as high as 26 for large cleaved samples close to large metallic electrodes. Our samples differ from others in this respect as well. Because of the small size of our mesas, $1/k$ is small, keeping the electromagnetic fields well confined and away from large metallic objects such as the ground plane beneath the sample. Using a solution for $\bar{\epsilon}$ for a sample in the proximity of metal plates,[12] we find that this ground plane distorts the value of $\bar{\epsilon}$ by less than 5% in our geometry. Even a hypothetical metal plate 300 μm above the sample surface changes $\bar{\epsilon}$ by less than 2%. This provides an upper limit to the distortions that may be caused by two 25-μm-diam wire that loop at this distance towards the center σ_{xx} contacts. For similar reasons, we expect the small, 10-μm-wide pulser and detector to have little effect on $\bar{\epsilon}$.

Figure 4(a) shows $\mathrm{Im}(l)$ and $|l|$ as determined from ω and ω' in Fig. 3 using Eq. (1) with $\bar{\epsilon}=7$. $|l|\approx\mathrm{Im}(l)$ over most of the graph as $\mathrm{Re}(l)\ll\mathrm{Im}(l)$ except at integer filling fractions. Figure 4(a) also shows $\mathrm{Im}(l)$ determined from Eq. (2), replacing $\sigma_{xx}(\omega)$ with $\sigma_{xx}(0)$ and the same value for $\bar{\epsilon}$. There is rather good agreement between these two curves in the regions between minima but poor overlap at the minima. The agreement worsens as $\bar{\epsilon}$ deviates from 7. For instance, choosing $\bar{\epsilon}=8$ decreases the value of $\mathrm{Im}(l)$ derived from Eq. (1) by about a factor of 2, whereas the value of $\mathrm{Im}(l)$ predicted by Eq. (2) decreases by only 12%. The data, in conjunction with VM's theory, thus suggests an $\bar{\epsilon}$ of 7.

In deriving $\mathrm{Im}(l)$ from Eq. (2), we have used $\sigma_{xx}(\omega)=\sigma_{xx}(0)$. This approximation needs to be justified. Expanding the conductivity about zero frequency, one finds that in the limit $\omega\ll\omega_c$ and $\omega\tau\ll1$ (where τ is the momentum relaxation time) $\mathrm{Re}[\sigma_{xx}(\omega)]\approx\mathrm{Re}[\sigma_{xx}(0)]$ and $\mathrm{Im}[\sigma_{xx}(\omega)]\approx\omega\tau\,\mathrm{Re}[\sigma_{xx}(0)]$, and hence, according to Eq. (2),

$$\mathrm{Re}(l)\approx\omega\tau\,\mathrm{Im}(l)\,. \tag{3}$$

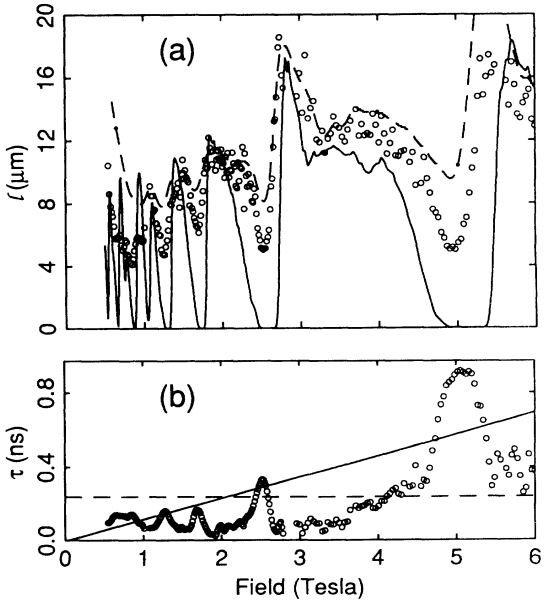

FIG. 4. (a) $\mathrm{Im}(l)$ (circles) and $|l|$ (dashed curve) as obtained from the data of Fig. 3 using Eq. (1) and $\bar{\epsilon}=7$. The solid curve is $\mathrm{Im}(l)$ derived from Eq. (2). (b) Momentum relaxation time determined from the data of Fig. 3 using Eq. (3). The dashed line is the mobility scattering time, and the solid line demarcates $\omega\tau=1$.

We can therefore obtain $\tau(B)$ from Eq. (3). The result is shown in Fig. 4(b) together with a solid line representing $\omega\tau \approx 1$. For $\tau(B)$ well below this line, our approximation should hold and we should expect areas of good agreement between the dotted and the solid curves in Fig. 4(a), as is indeed the case. On the other hand, the value of τ as well as that of l derived from Eq. (2) are unreliable where $\tau(B)$ approaches or exceeds this line. For comparison we also show in Fig. 4(b) the elastic-scattering time determined from dc mobility measurements. It is satisfying to find that our results for $\tau(B)$ fall within a factor of 5 of this value.

Referring back to Fig. 4(b), we note that the boundary layer width $|l|$ never becomes smaller than about 7 μm. This contrasts with the results of the GHvK (Ref. 10) study which give values of $|l|$ as narrow as 50 nm. The enormous discrepancy between the GHvK determination of $|l|$ and ours arises from the exceptionally high value of $\bar{\epsilon} \approx 20$ which these authors employ. Using $\bar{\epsilon} = 20$, we also obtain much smaller minimum values for $|l|$; however, our sample geometry and the good agreement between the curves in Fig. 4(a) do not prescribe the use of such a large dielectric constant.

What is the meaning of the apparent lower bound on the boundary layer width? In the context of Eq. (2), this bound may arise because the complex conductivity of the 2DEG at our high frequencies ω never drops below a certain value. Alternatively, VM's model for $|l|$ in Eq. (2) may fail when it predicts very small values $|l|$. Indeed, Shikin[16] has argued that the Larmor radius may act as a lower bound on $|l|$. There may exist yet another bound. The VM theory was developed for a 2DEG in which the conductivity and density drop abruptly to zero at the sample edge. In reality, there must exist a healing length over which the 2DEG moves from full depletion to bulk density. This is expected to be a slow $1/x$ process[17] with a characteristic length of the order 1 μm. The healing length of the 2DEG may place a rather large lower bound on the length $|l|$ as is seen in the analysis of our data. Finally, we again point out the limited validity of the VM model in the QHE regime and note that an analysis of the EMP data considering the nonlocality of the transport coefficients in the QHE may yield different values for $|l|$.

We are grateful to H. Baranger, J. Eisenstein, L. Glazman, T. Gramila, A. Levi, P. Littlewood, and R. Nottenburg for helpful conversations.

[1]S. J. Allen, H. L. Stormer, and J. C. M. Hwang, Phys. Rev. B **28**, 4875 (1983).

[2]D. B. Mast, A. J. Dahm, and A. L. Fetter, Phys. Rev. Lett. **54**, 1706 (1985).

[3]D. C. Glattli, E. Y. Andrei, G. Deville, J. Poitrenaud, and F. I. B. Williams, Phys. Rev. Lett. **54**, 1710 (1985).

[4]E. Y. Andrei, D. C. Glatti, F. I. B. Williams, and M. Heiblum, Surf. Sci. **196**, 501 (1988).

[5]V. I. Talyanskii, Pis'ma Zh. Eksp. Teor. Fiz. **43**, 96 (1985) [JETP Lett. **43**, 127 (1986)].

[6]V. A. Volkov. D. V. Galchenkov, L. A. Galchenkov, I. M. Grodnenskii, O. R. Matov, and S. A. Mikhailov, Pis'ma Zh. Eksp. Teor. Fiz. **44**, 510 (1986) [JETP Lett. **44**, 655 (1986)].

[7]T. Demel, D. Heitmann, P. Grambow, and K. Ploog, Phys. Rev. Lett. **64**, 788 (1990).

[8]V. K. Talyanskii, M. Wassermeier, A. Wixforth, J. Oshinowo, J. P. Kotthaus, I. E. Batov, G. Weimann, H. Nickel, and W. Schlapp, Surf. Sci. **229**, 40 (1990).

[9]M. Wassermeier, J. Oshinowo, J. P. Kotthaus, A. H. MacDonald, C. T. Foxon, and J. J. Harris, Phys. Rev. B **41**, 10287 (1990).

[10]I. Grodnensky, D. Heitmann, and K. von Klitzing, Phys. Rev. Lett. **67**, 1019 (1991).

[11]X. G. Wen, Phys. Rev. Lett. **64**, 2206 (1990).

[12]V. A. Volkov and S. A. Mikhailov, Zh. Eksp. Teor. Fiz. **94**, 217 (1988) [Sov. Phys. JETP **67**, 1639 (1988)].

[13]A. H. MacDonald, Phys. Rev. Lett. **64**, 220 (1990).

[14]J. K. Wang and V. J. Goldman, Phys. Rev. Lett. **67**, 749 (1991).

[15]V. A. Volkov and S. A. Mikhailov, Pis'ma Zh. Eksp. Teor. Fiz. **42**, 450 (1985) [JETP Lett. **42**, 556 (1985)].

[16]V. B. Shikin, Pis'ma Zh. Eksp. Teor. Fiz. **47**, 471 (1988) [JETP Lett. **47**, 555 (1988)].

[17]L. I. Glazman and I. A. Larkin, Semicond. Sci. Technol. **6**, 32 (1991).